Available online at www.sciencedirect.com
SCIENCE DIRECT
Journal of Catalysis 237 (2006) 67–78
JOURNAL OF CATALYSIS
www.elsevier.com/locate/jcat

Experimental evidence for a significant homometallic catalytic binuclear elimination reaction: Linear-quadratic kinetics in the rhodium catalyzed hydroformylation of cyclooctene

Guowei Liu, Chuanzhao Li, Liangfeng Guo, Marc Garland *

Department of Chemical and Biomolecular Engineering, 4 Engineering Drive 4, National University of Singapore, Singapore 119260

Received 14 July 2005; revised 29 September 2005; accepted 29 September 2005

Available online 23 November 2005

Abstract

The hydroformylation of cyclooctene was studied using $Rh_4(CO)_{12}$ as precursor in *n*-hexane solvent in the temperature range 293–308 K and P_T of 4.0–8.0 MPa, using quantitative in situ infrared spectroscopy. During the course of reaction, the degradation of $Rh_4(CO)_{12}$ to the intermediate $RCORh(CO)_4$ was observed, with accompanying formation of cyclooctane carboxaldehyde. The limited conversion of $Rh_4(CO)_{12}$ to $RCORh(CO)_4$ was shown to be equilibrium-controlled. Some ketone was also formed. Spectral deconvolution was performed with band-target entropy minimization (BTEM). The reaction kinetics for product formation, in terms of the observable organometallics, were rate $= k_1[RCORh(CO)_4][CO]^{-1}[H_2] + k_2[RCORh(CO)_4][Rh_4(CO)_{12}]^{0.25}[H_2]^{0.5}[CO]^Y$. This can be rewritten as rate $= k_1[RCORh(CO)_4][CO]^{-1} \times [H_2] + k_2[RCORh(CO)_4][HRh(CO)_4][CO]^X$. The hydride $HRh(CO)_4$ could be identified by BTEM but not accurately quantified. This unusual linear-quadratic expression in rhodium species represents the kinetic form for a simultaneous interconnected unicycle catalytic mechanism and a homometallic catalytic binuclear elimination reaction (CBER). The second term accounted for ca. 40% of the observed product formation at the mean reaction conditions used in this study. The implications and opportunities presented by homometallic CBER are discussed. In particular, a form of modified homometallic CBER is proposed that will permit greater utilization of the nonlinear kinetics.

Keywords: Catalytic binuclear elimination reaction; Linear-quadratic kinetics; Rhodium-catalyzed hydroformylation; In situ quantitative FTIR spectroscopy

1. Introduction

One of the most widely studied transition metal homogeneous catalyzed reactions [1,2], the hydroformylation reaction provides a versatile route for the synthesis of a vast array of bulk and specialty chemicals [3]. The primary transition metals used are cobalt [4], rhodium [5], and platinum [6].

Because of the versatility of this reaction, a very wide range of unfunctionalized and functionalized alkenes have been used as substrates [7]. In the case of unfunctionalized rhodium-catalyzed hydroformylation, comparisons of activity (reaction rates) have been studied in detail for various classes of unmodified alkene substrates [8–13], and significant variation has been found. In situ studies of the unmodified rhodium-catalyzed hydroformylation of unfunctionalized alkenes has revealed that although the rates are substantially different between classes, the turnover frequencies (TOFs), based on the instantaneous concentrations of the observable acyl intermediate are for the most part very similar [14–17]. This indicates a wide variability in the conversion of precursor to intermediates. In addition, a fair number of anomalies in activity or selectivity patterns have been observed; for example, (1) in the case of ethylene, the corresponding ketone is frequently formed [18,19]; (2) in the case of cyclohexene, unusually high CO pressures are needed to form the acyl complex; (3) for some cycloalkenes, there is very low equilibrium-controlled precursor conversion [16]; and (4) in the case of methylene cyclopropane, ring cleavage occurs [20].

The observation of anomalous substrate behaviors, even within a homologous series of substrates, is not restricted to the hydroformylation reaction alone. Indeed, other well-studied

* Corresponding author. Fax: +65 6 779 1936.
E-mail address: chemvg@nus.edu.sg (M. Garland).

0021-9517/$ – see front matter
doi:10.1016/j.jcat.2005.09.033

catalytic reactions, such as hydrogenation, have numerous documented examples [21]. The primary issue to emphasize is that further study of the origins of these anomalous observations is infrequently pursued. The eventual clarification of the underlying mechanisms behind the anomalous observations of activity and selectivity may provide rich scientific opportunities.

The study of binuclear elimination, and even catalytic binuclear elimination, has been gaining interest over the past few decades. These studies have been driven in part by the need to explain anomalous activity and selectivity patterns. Presently, there are ca. 14 well-defined homometallic stoichiometric binuclear elimination reactions (Table 1). Of course, the existence of homometallic stoichiometric binuclear elimination reactions raises the issue of related catalytic possibilities. Such a mechanism would provide the basis for a catalytic binuclear elimination reaction (CBER).

The cobalt-mediated hydroformylation reaction represents the best example of both stoichiometric and catalytic investigations. The reaction of acyl cobalt tetracarbonyls with cobalt tetracarbonyl hydride was first reported by Heck and Breslow [25], then extensively investigated by the Vesprem group [26–28]. Both groups suggested that a catalytic analog to stoichiometric CBER may be present in addition to a unicyclic topology during cobalt-catalyzed hydroformylations. The possible presence of CBER was further suggested by in situ spectroscopy of the cobalt-catalyzed hydroformylation [41]. In 1983, Mirbach conducted an in situ infrared IR study of the homogeneous cobalt-catalyzed hydroformylation of 1-octene and found that perhaps 4% of the product formation arose from a homometallic CBER [42].

Based on studies of the elimination mechanism of osmium alkyls and osmium hydrides, Norton suggested that binuclear elimination is probably much more common than has been realized, because of the extraordinary ability of metal hydrides to fill vacant coordination sites on other metals [30]. He also argued that binuclear elimination is probably involved to some extent in the cobalt-catalyzed oxo reaction. In his later work on the relative nucleophilicity of metal hydrides, Norton further indicated that binuclear elimination could be the terminal step in catalytic hydroformylation [37].

In addition, in the studies of a surface-tethered silica-supported rhodium hydroformylation of styrene, Collman et al. [43] found a nonlinear rate dependence of the hydroformylation of styrene with the surface concentration of the rhodium catalyst species. Accordingly, these authors discussed the possibility of dinuclear reductive elimination as the site–site interaction [43].

An in situ spectroscopic attempt to identify a homometallic CBER in the unmodified homogeneous rhodium-catalyzed hydroformylation reaction was conducted in 1999 [44]. In that study, cyclohexene was used as a substrate, because the known equilibrium-controlled precursor conversion would result in only ca. 10% conversion of $Rh_4(CO)_{12}$ at 6.0 MPa CO partial pressure. Thus the catalytic system should contain considerable quantities of $HRh(CO)_4$ in equilibrium with $Rh_4(CO)_{12}$ in addition to the $RCORh(CO)_4$ present, and hence the probability of binuclear elimination between $HRh(CO)_4$ and $RCORh(CO)_4$ should be nonnegligible. However, no statistical evidence of a homometallic CBER could be found. It is worth mentioning that no spectroscopic evidence for the presence of observable quantities of $HRh(CO)_4$ could be obtained in that study, most likely due to the lack of appropriate signal processing tools at that time.

The development of band-target entropy minimization (BTEM) [45–50] and associated algebraic tools [51] has made it possible to conduct more detailed in situ studies. Recently we obtained strong evidence for *bimetallic* CBER kinetics in the rhodium-catalyzed hydroformylation of 3,3-dimethyl-but-1-ene and cyclopentene promoted with $HMn(CO)_5$ [52,53]. This prompted renewed interest in anomalous homometallic rhodium hydroformylation. Because the rhodium-catalyzed hydroformylation of cyclooctene is also known to exhibit equilibrium-controlled precursor conversion, we have reinvestigated the rhodium-catalyzed hydroformylation of cyclooctene in an attempt to better understand the kinetics [54]. The present paper reports this effort and our conclusion that a significant homometallic CBER is present.

2. Experimental

2.1. General information

All solution preparations and transfers were carried out under purified argon (99.9995%, Saxol; Singapore) atmosphere using standard Schlenk techniques [55]. The argon was further purified before use by passing it through a deoxy and zeolite column. Purified carbon monoxide (research grade, 99.97%, Saxol; Singapore) and purified hydrogen (99.9995%, Saxol; Singapore) were also further purified through deoxy and zeolite columns before being used in the hydroformylation experiments. Purified nitrogen (99.9995%, Saxol; Singapore) was used to purge the Perkin–Elmer 2000 Fourier transform infrared (FTIR) spectrometer system.

$Rh_4(CO)_{12}$ (98%) was purchased from Strem Chemicals and was used without further purification. The cyclooctene (99.9%, Chemsampco) was dehydrated with CaH_2 before use and stored under argon in a refrigerator. After dehydrating, no other species could be detected by GC (HP6890; HP-FFAP polyethylene glycol TPA capillary column, 100 °C; flame ionization detector, 250 °C).The puriss-quality *n*-hexane (99.6%; Fluka) was distilled from sodium-potassium alloy under argon for ca. 5 h to remove trace water and oxygen.

2.2. Apparatus

In situ kinetic studies were performed in a 1.5-L stainless-steel (SS316) autoclave ($P_{max} = 22.5$ MPa; Buchi–Uster), connected to a high-pressure IR flow cell. The system is the same as that used in earlier studies [14–17], and a schematic diagram of the experimental setup has been provided previously [17].

2.3. In situ spectroscopic and kinetic studies

A total of 16 kinetic experiments in 5 sets were performed. In each set, one experimental parameter was systematically

Table 1
Presently known homometallic stoichiometric binuclear elimination reactions

No	Reaction	Reference
1	$2HCo(CO)_4 \rightarrow Co_2(CO)_8 + H_2$	[22,23]
2	$2HMn(CO)_5 \rightarrow Mn_2(CO)_{10} + H_2$	[24]
3	$RCOCo(CO)_4 + HCo(CO)_4 \rightarrow Co_2(CO)_8 + RCHO$	[25–27]
4	$RCo(CO)_4 + HCo(CO)_4 \rightarrow Co_2(CO)_8 + RH$	[28]
5	$2Os(CO)_4H_2 \rightarrow H_2Os_2(CO)_8 + H_2$	[29–31]
6	$2Os(CO)_4(H)CH_3 \rightarrow HOs(CO)_4Os(CO)_4CH_3 + CH_4$	[29–31]
7	$Os(CO)_4H_2 + Os(CO)_4(CH_3)_2 \rightarrow HOs(CO)_4Os(CO)_4CH_3 + CH_4$	[29–31]
8	$Os(CO)_4H_2 + Os(CO)_4(H)CH_3 \rightarrow H_2Os_2(CO)_8 + CH_4$	[29–31]
9	$RMn(CO)_5 + HMn(CO)_5 \rightarrow Mn_2(CO)_9 + RCHO$	[32–34]
10	$2HRh(CO)_2(PPh_3)_2 \rightarrow Rh_2(CO)_2(PPh_3)_2 + H_2 + 2CO$	[35]
11	$2HIr(CO)(PPh_3)_3 \rightarrow Ir_2(CO)_2(PPh_3)_4 + H_2 + 2PPh_3$	[36]
12	$EtRe(CO)_5 + HRe(CO)_5 \rightarrow EtCHO + Re_2(CO)_9$	[37]
13	$EtHFe(CO)_4 + CH_3CH_2C(=O)FePPh_3(CO)_3 \rightarrow CH_3CH_2CHO + EtFe_2PPh_3(CO)_7$	[38]
14	$(\eta^5\text{-}C_5H_5)Mo(CO)_3H + (\eta^5\text{-}C_5H_5)Mo(CO)_3R \rightarrow (\eta^5\text{-}C_5H_5)_2Mo_2(CO)_4 + RCHO + CO$	[39,40]

Table 2
Experimental design for the $Rh_4(CO)_{12}$ catalyzed hydroformylation of cyclooctene

Experiment	CO (MPa)	H_2 (MPa)	Cyclooctene (mL)	$Rh_4(CO)_{12}$ (mg)	Temperature (K)
Standard	4.0	2.0	10	100.1	298.0
CO	2.0	2.0	10	99.9	298.0
variation	3.0	2.0	10	99.9	298.0
	5.0	2.0	10	103.2	298.0
H_2 variation	4.0	1.0	10	105.2	298.0
	4.0	3.0	10	104.0	298.0
	4.0	4.0	10	98.2	298.0
Cyclooctene	4.0	2.0	5	100.7	298.0
variation	4.0	2.0	15	100.9	298.0
	4.0	2.0	20	98.8	298.0
$Rh_4(CO)_{12}$	4.0	2.0	10	50.5	298.0
variation	4.0	2.0	10	198.7	298.0
	4.0	2.0	10	255.3	298.0
Temperature	4.0	2.0	10	100.2	293.0
variation	4.0	2.0	10	100.1	303.0
	4.0	2.0	10	101.6	308.0

varied while the remaining variables were kept essentially constant. The detailed experimental design for this study is given in Table 2. The experimental design of the experiments involved 300 mL of solvent and the following intervals: temperature, 293–308 K; P_{H_2}, 1.0–4.0 MPa; P_{CO}, 2.0–5.0 MPa; initial alkene, 5–20 mL; and initial $Rh_4(CO)_{12}$, 50.5–255.3 mg.

All of the experiments were performed in a similar manner. A typical procedure for the standard experiment was as follows. First, background spectra of the IR sample chamber were recorded. Then 150 mL of *n*-hexane was transferred under argon to the autoclave. Under 0.2 MPa CO pressure, IR spectra of the *n*-hexane in the high-pressure cell were recorded. The total system pressure was raised to 4.0 MPa CO, and the stirrer and high-pressure membrane pump were started. After equilibration, IR spectra of the CO/*n*-hexane solution in the high-pressure cell were recorded. A solution of 10 mL of cyclooctene dissolved in 50 mL of *n*-hexane was prepared, transferred to the high-pressure reservoir under argon, pressurized with CO, and then added to the autoclave. After equilibration, IR spectra of the cyclooctene CO/*n*-hexane solution in the high-pressure cell were recorded. A solution of ca. 100 mg of $Rh_4(CO)_{12}$ dissolved in 50 mL of *n*-hexane was prepared, transferred to the high-pressure reservoir under argon, pressurized with CO, and then added to the autoclave. After equilibration, IR spectra of the $Rh_4(CO)_{12}$/cyclooctene/CO/*n*-hexane solution in the high-pressure cell were recorded. After this, 2.0 MPa of hydrogen was added to initiate the synthesis.

The in situ spectra were obtained every 15 min during each 6-h experiment in the range of 1000–2500 cm^{-1} with a resolution of 4 cm^{-1}. A total of 320 spectra were obtained for further spectroscopic and kinetic analyzes.

Two relevant reviews on in situ IR spectroscopic studies of general catalytic systems [56] and in situ IR spectroscopic studies of the hydroformylation reaction [57] have recently appeared.

2.4. Transport considerations

The primary transport issues to consider in a homogeneous catalytic reaction being monitored by in situ spectroscopy are (1) the mixing times in the continuous-stirred tank reactor (CSTR) and recycling system, (2) the rate of gas–liquid mass transfer compared with the rate of reaction, and (3) the extent of reaction occurring outside the CSTR and inside the recycle loop (i.e., the composition difference between outlet and inlet). A review of these issues and the associated calculations have been provided previously [58]. The mixing time in the CSTR and recycling loop was on the order of a few minutes. The experimentally measured overall mass transfer coefficients, K_La, for hydrogen and carbon monoxide into *n*-hexane at 200 rpm were approximately 0.1 and 0.06 s^{-1}, respectively. Taking into account the gas solubility at the mean reaction conditions, the maximum rates of mass transfer were ca. 3×10^{-3} mol fraction/s. Because the maximum observed rate of hydroformylation in this study was ca. 3.5×10^{-7} mol fraction/s, all hydroformylation experiments exhibited product formation rates belonging to the category H of Hatta classifications—infinitely slow reaction compared with gas–liquid mass transfer. Saturation at

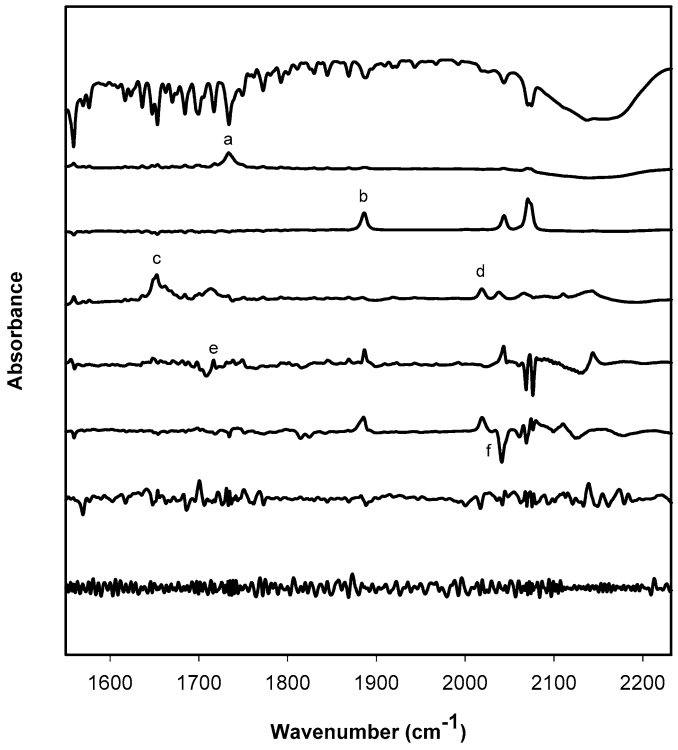

Fig. 1. A singular value decomposition of the in situ spectroscopic data showing the 1st, 2nd, 4th, 7th, 12th, 19th, 50th significant vectors and the 320th vector. The labeled extrema are those which were used to recover the pure organometallic component spectra as well as alkene and aldehyde by BTEM. The reaction conditions are $P_{CO} = 2.0$–5.0 MPa, $P_{H_2} = 1.0$–4.0 MPa, cyclooctene = 5–20 mL, $Rh_4(CO)_{12}$ = 50.5–255.3 mg in 300 mL *n*-hexane at 298 K.

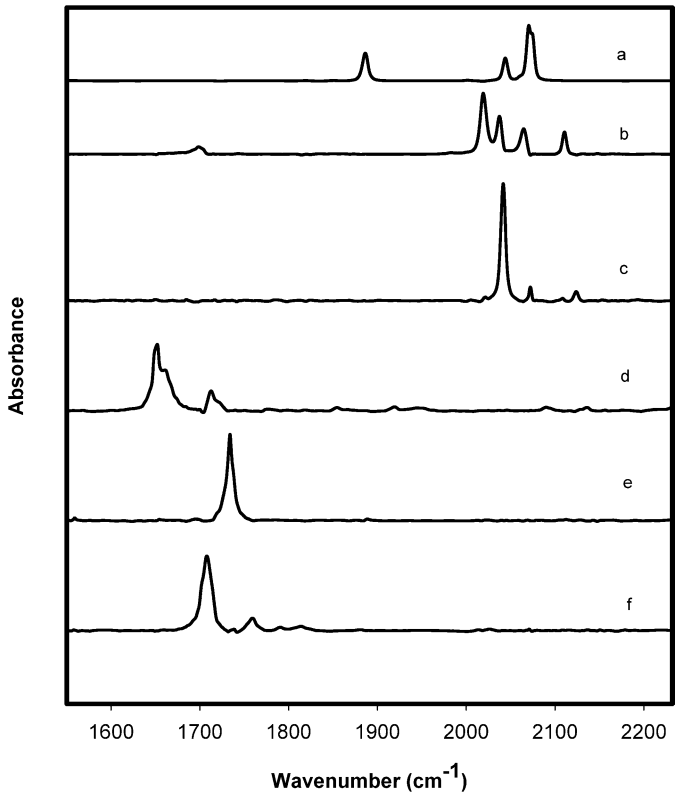

Fig. 2. The recovered pure component spectra of the organic and organometallic species using BTEM: (a) $Rh_4(CO)_{12}$, (b) $RCORh(CO)_4$, (c) $HRh(CO)_4$, (d) cyclooctene, (e) cyclooctane carboxaldehyde, and (f) ketone. The reaction conditions are $P_{CO} = 2.0$–5.0 MPa, $P_{H_2} = 1.0$–4.0 MPa, cyclooctene = 5–20 mL, $Rh_4(CO)_{12}$ = 50.5–255.3 mg in 300 mL *n*-hexane at 298 K.

the beginning of a run was achieved on the order of a few minutes. The mixing issues together with the initial gas–liquid mass transfer issue indicate that transport effects influence the first few minutes of reaction. The residence time in the recycle loop was on the order 2 min. The concentrations of the reagents dissolved CO, H_2, and cyclooctene varied by <1% along the recycling loop during this period. Accordingly, the concentrations of these components as well as the organometallics at the spectrometer are only differentially removed from the concentrations within the CSTR, and thus the measurements are truly in situ.

2.5. Computations

The newly developed algorithms of BTEM for spectral deconvolution and algebraic system identification for catalytic reaction modeling were used to analyze the in situ IR spectra [45–51].

3. Results

3.1. Spectroscopic aspects

The 320 in situ FTIR spectra in this experimental study were analyzed over the spectral interval 1550–2230 cm^{-1} with data intervals of 0.2 cm^{-1}. Fig. 1 shows notable vectors from the singular value decomposition of the spectroscopic matrix $\mathbf{A}_{320\times3401}$. These vectors contain the chemically important spectral features for the pure component spectra. Fig. 2 shows the correspondingly recovered pure component spectra obtained from the BTEM analysis (solvent hexane, atmospheric moisture, and CO_2 and dissolved CO are omitted).

Fig. 2 shows that the reconstructed pure component spectra are consistent with those obtained in the numerous previous in situ FTIR spectroscopic studies of the unmodified rhodium-catalyzed hydroformylation of alkenes [14–17,44–51]. These studies have shown that the rhodium precursors are transformed under reaction conditions to generate observable quantities of a mononuclear acyl complex, namely $RCORh(CO)_4$, with characteristic features at 1698, 2020, 2039, 2065, and 2111 cm^{-1}. To date, approximately 20 acyl rhodium tetracarbonyl complexes have been observed in situ [20], but evidence for observable quantities of other intermediates has been exceptionally difficult to obtain. The most obvious coordinately saturated 18e-mononuclear species expected under hydroformylation conditions are the hydride $HRh(CO)_4$ [59,60] and the alkyl $RRh(CO)_4$. Spectroscopic evidence of the existence of the former under syngas has developed over the years, and outstanding spectra of both $HRh(CO)_4$ [2002.8(vw), 2041.6(vs), 2071.8(m), 2123.6(vw) cm^{-1}] and $DRh(CO)_4$ were obtained recently [48]. However, analyzes of spectra from active unmodified hydroformylations have not conclusively indicated observable quan-

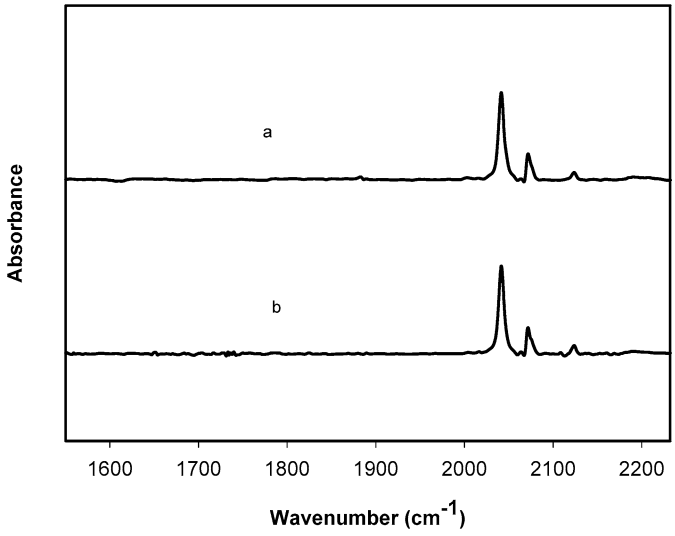

Fig. 3. The target and projected pure component spectra of $HRh(CO)_4$: (a) target vector and (b) projected vector. The reaction conditions are P_{CO} = 2.0–5.0 MPa, P_{H_2} = 1.0–4.0 MPa, Cyclooctene = 5–20 mL, $Rh_4(CO)_{12}$ = 50.5–255.3 mg in 300 mL *n*-hexane at 298 K.

tities of $HRh(CO)_4$ until now. The spectrum of $HRh(CO)_4$ was recoverable in the present study.

The resolved spectrum is a little distorted, although the primary bands at ca. 2042, 2071, and 2123 cm^{-1} could be recovered. Some random signals associated with measurement noise are observed. In addition, target factor analysis (TFA) [61] was performed to provide independent confirmation of $HRh(CO)_4$. A pure component spectrum of $HRh(CO)_4$ obtained from a noncatalytic experiment in this laboratory was used as the target vector and was projected onto 50 vectors of the V^T matrix. Fig. 3 shows the target and projected pure component spectra. These results indeed confirm the presence of the component at very low concentration. The projected vector has a good signal-to-noise ratio of >25:1.

In most investigations of hydroformylation reactions, the corresponding aldehyde is by far the predominant overall organic product, particularly when rhodium is used. However, sometimes ketone and even polyketone formation is nonnegligible [18,19]. In the present experiments, ketone formation occurred as confirmed by the spectral feature at 1720 cm^{-1}.

Table 3 gives the contributions of each component to the spectral absorbance, as well as the total percentage of signal recovery. The contribution of moisture to the total signal in this 1999 experimental dataset was a very significant 27.49%. Our later studies show significantly less moisture in the FTIR spectra. Such a large contribution of moisture, with its sharp and nonstationary bands, puts considerable restrictions on the spectral recovery and total percentage of signal that can be modeled. Despite this difficulty, however, ca. 99% of the signal could be modeled. The total signal associated with the organometallics was only ca. 2.8%.

In the interest of completeness, it should be mentioned that the presence of trace amounts of conjugated 1,3-cyclooctadiene in the cyclooctene substrate cannot be excluded. (Conjugated dienes are common impurities in cycloalkenes.) As shown previously [62], the presence of conjugated dienes in rhodium-catalyzed hydroformylations often results in a new characteristic metal–carbonyl vibration at ca. 1992 cm^{-1}. A weak local extremum at 1992 cm^{-1} was observed in the V^T vectors of this study, but pure component spectral recovery was unsuccessful.

Table 3
Percentage of integrated absorbance for each component compared to the total original experimental data

Component	Integrated intensity of each component (%)
Moisture	27.49
n-hexane	33.65
Dissolved CO	31.58
$Rh_4(CO)_{12}$	2.26
$C_8H_{15}CHO$	2.09
Cyclooctene	0.89
$RCORh(CO)_4$	0.50
Ketone	0.44
$HRh(CO)_4$	0.08
$Rh_6(CO)_{16}$	[a]
Total	98.98

[a] Negligible contribution. Pure component spectrum not recoverable but presence verified by TTFA.

3.2. Representative experiments and kinetics

The 16 experiments provided 5 distinct subsets, which were then analyzed for precursor conversion and organic product formation. In what follows, to save space, we summarize the results of the equilibrium conversion and present only the rhodium series in their entirety. The remaining results can be found in the supporting information.

3.2.1. The rhodium variation experiments

The set of experiments associated with the variations in rhodium were all conducted with the initial conditions of 4.0 MPa CO, 2.0 MPa hydrogen, and 10 mL cyclooctene in 300 mL *n*-hexane at 298 K. The initial amounts of rhodium precursor $Rh_4(CO)_{12}$ were 52.6, 102.1, 199.8, and 253.3 mg.

3.2.1.1. Precursor conversion Fig. 4 shows the mole fractions of the catalyst precursor and the one and only quantifiable mononuclear intermediate, $RCORh(CO)_4$, as a function of time. The time series show very little scatter in the mole fraction data. As seen in this figure, the precursor and $RCORh(CO)_4$ rapidly achieved a more-or-less steady-state situation in ca. 30 min. The percent conversion for these four experiments was ca. 20.9, 12.0, 7.6, and 6.3%. Fig. 4 indicates that the formation of $RCORh(CO)_4$ and disappearance of $Rh_4(CO)_{12}$ are consistent with a good mass balance on rhodium. A small increase in the concentration of $Rh_4(CO)_{12}$ and a small decrease in the concentration of $RCORh(CO)_4$ occurred over time due to consumption of the substrate.

3.2.1.2. Aldehyde Fig. 5 shows the mole fractions of the aldehyde product as a function of time. Again, the time series show very little scatter in the mole fraction data. A small induction period occurred in the first 30 min of each series. The rates

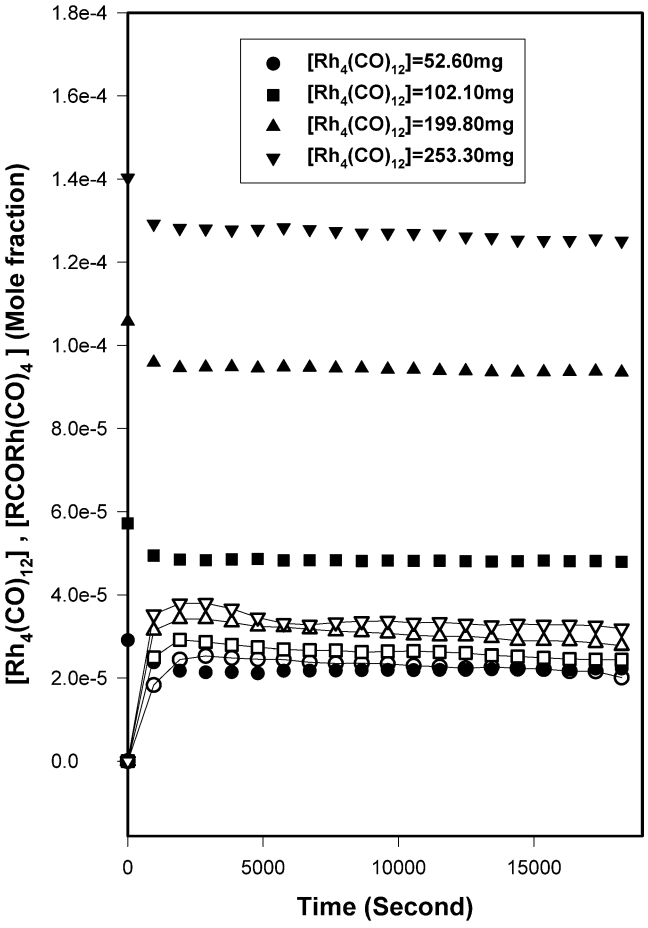

Fig. 4. Time series data for the primary quantifiable organorhodium species present during the rhodium variation set of experiments. The data points with line represent $RCORh(CO)_4$, while those without line represent $Rh_4(CO)_{12}$. The remaining reaction conditions are held constant at $V_{alkene} = 10$ mL, $P_{CO} = 4.0$ MPa, $P_{H_2} = 2.0$ MPa, at 298 K.

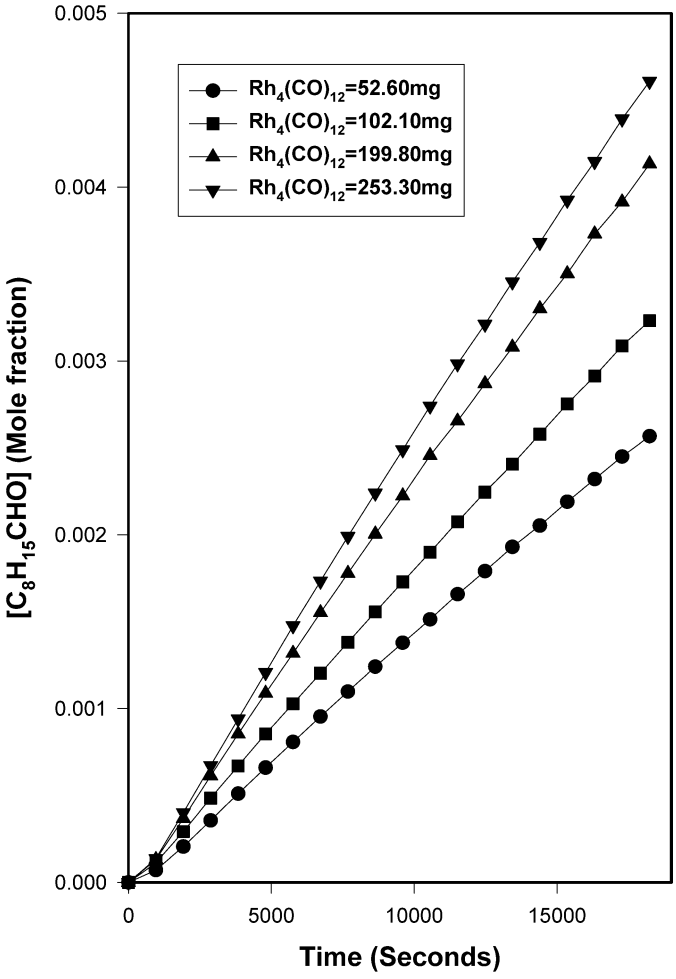

Fig. 5. Time series data for the organic product $C_8H_{15}CHO$ present during the rhodium variation set of experiments. The remaining reaction conditions are held constant at $V_{alkene} = 10$ mL, $P_{CO} = 4.0$ MPa, $P_{H_2} = 2.0$ MPa, at 298 K.

of reaction for these four experiments were ca. 1.4×10^{-7}, 1.8×10^{-7}, 2.3×10^{-7}, and 2.6×10^{-7} mol fraction/s.

3.2.1.3. Turnover frequency Fig. 6 shows the TOFs for aldehyde formation based on the instantaneous mole fractions of $RCORh(CO)_4$ in each experiment as a function of $Rh_4(CO)_{12}$ loading and as a function of time. These time series data demonstrate increased scatter due to the fact that two independent experimental observations are needed for each data point. Regression of the data for each run provided the values TOF (52.60 mg) $= (6.20 \pm 0.16) \times 10^{-3}$ s^{-1}, TOF (102.10 mg) $= (6.85 \pm 0.10) \times 10^{-3}$ s^{-1}, TOF (199.80 mg) $= (7.50 \pm 0.09) \times 10^{-3}$ s^{-1}, and TOF (253.30 mg) $= (7.93 \pm 0.57) \times 10^{-3}$ s^{-1}, where the errors were listed as twice the standard deviation (i.e., 95% confidence limit). Clearly, TOF is not a constant; it increases with increased loading of $Rh_4(CO)_{12}$.

Previous studies of unmodified rhodium-catalyzed hydroformylations of 3,3-dimethyl-but-1-ene have repeatedly shown that TOF is a function of temperature, hydrogen pressure, and carbon monoxide pressure [15,52]. The present results clearly show that TOF is also dependent on rhodium loading. This is not expected for a unicycle catalytic mechanism, which has rates linear in the total concentration of intermediates. The observed nonlinear aspects of TOF indicate the possible contribution of a CBER to the final product formation.

3.3. Analysis of precursor conversion

The precursor $Rh_4(CO)_{12}$ should be equilibrated with the hydride species $HRh(CO)_4$, and this species should be equilibrated with its coordinately unsaturated hydride, $HRh(CO)_3$. As derived previously [16], a steady-state assumption can be imposed on the concentration of $HRh(CO)_3$ in terms of its disappearance due to alkene coordination and its formation due to hydrogenolysis of the acyl complex. This results in an expression for *equilibrium-controlled* precursor formation in unmodified rhodium-catalyzed hydroformylations of the form in Eq. (1), where the subscript denotes steady-state concentrations. In the hydroformylation of cyclohexene, the experimentally determined relationship was that of Eq. (2) [16], where $[Rh_4(CO)_{12}]$, [CO], $[H_2]$, and $[R']$ represent the mole fractions of precursors, dissolved gases, and substrate used:

$$[RCORh(CO)_4]_{SS} = \Phi[Rh_4(CO)_{12}]_{SS}^{0.25}[CO][H_2]^{-0.5}[R']^1, \quad (1)$$

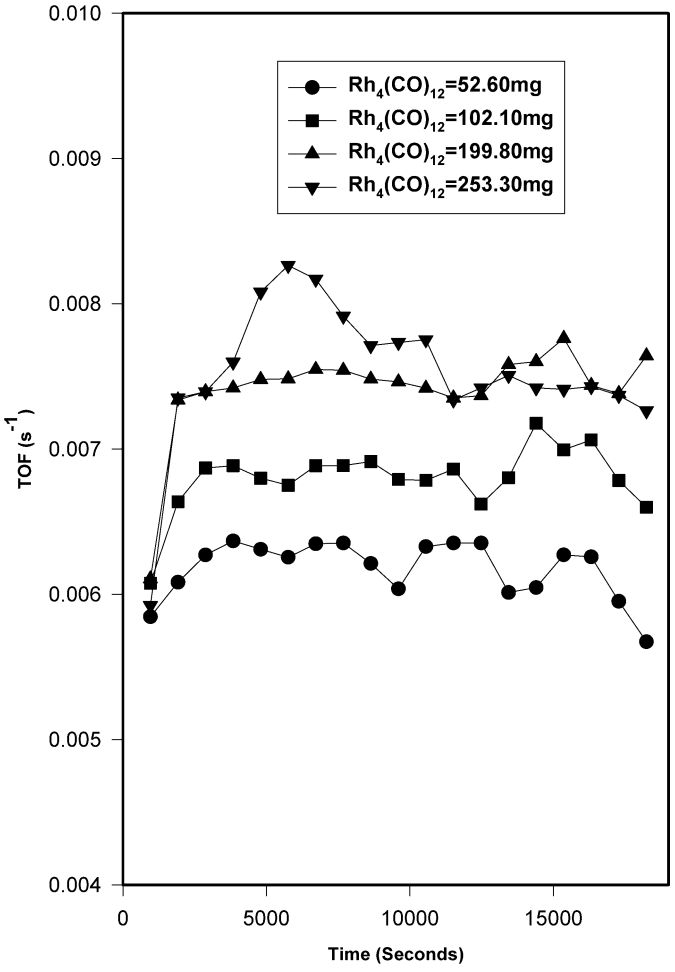

Fig. 6. The effects of $Rh_4(CO)_{12}$ loadings on the turnover frequencies (TOF) for aldehyde formation. The remaining reaction conditions were held constant at $V_{alkene} = 10$ mL, $P_{CO} = 4.0$ MPa, $P_{H_2} = 2.0$ MPa, at 298 K.

$$[\mathrm{RCORh(CO)_4}]_{SS} = \Phi[\mathrm{Rh_4(CO)_{12}}]_{SS}^{0.3}[\mathrm{CO}]^{1.1}[\mathrm{H_2}]^{-0.3}[\mathrm{R'}]^{0.9}. \quad (2)$$

In the present experimental study for the hydroformylation of cyclooctene, a multilinear regression was performed for the pseudo-steady-state concentration of the acyl rhodium tetracarbonyl in terms of the remaining reactants in the system (with all experimental runs used). The obtained relationship is given in Eq. (3). The values of the exponents have rather acceptable statistical bounds, so the data and regression appear to be rather good. The exponents are quite similar to those previously obtained experimentally in the case of cyclohexene and consistent with the hypothesis of equilibrium-controlled precursor conversion. In particular, the nuclearity difference between precursor and intermediate is clearly shown by the exponent of 0.23 for $Rh_4(CO)_{12}$:

$$[\mathrm{RCORh(CO)_4}]_{SS} = \Phi[\mathrm{Rh_4(CO)_{12}}]_{SS}^{0.23\pm0.1}[\mathrm{CO}]^{1.4\pm0.2} \times[\mathrm{H_2}]^{-0.3\pm0.2}[\mathrm{R'}]^{0.7\pm0.3}. \quad (3)$$

3.4. Analysis of catalytic kinetics

TOF analysis of the experimental data associated with the effect of initial $Rh_4(CO)_{12}$ (Fig. 6) suggests that a possible CBER exists in this system. In principle, the bimolecular reaction of $RCORh(CO)_3$ with molecular hydrogen is not the only mechanism available for the hydrogenolysis of $RCORh(CO)_4$. The possibility also exists that some aldehyde formation occurs via a bimolecular elimination reaction, similar to that found for the unmodified cobalt system under stoichiometric conditions [25], which is shown by

$$\mathrm{HCo(CO)_4 + RCOCo(CO)_{3,4} \rightarrow RCHO + Co_2(CO)_{7,8}}. \quad (4)$$

Under the experimental condition, there may exist several active species that could be involved in product formation, including $RCORh(CO)_3$, $RCORh(CO)_4$, $HRh(CO)_3$, $HRh(CO)_4$. In principle, both hydride rhodium species can react with both acyl rhodium species to yield aldehydes,

$$\mathrm{HRh(CO)_{3,4} + RCORh(CO)_{3,4} \rightarrow RCHO + Rh_2(CO)_{6,7,8}}. \quad (5)$$

We now state the working hypothesis that the experimental system consists of a simultaneous unicyclic reaction mechanism and a homometallic CBER. Accordingly, the rate of hydroformylation should take the general form

$$\mathrm{rate} = k_1[\mathrm{RCORh(CO)_4}][\mathrm{CO}]^{-1}[\mathrm{H_2}] + k_2[\mathrm{RCORh(CO)_4}][\mathrm{HRh(CO)_4}][\mathrm{CO}]^X. \quad (6)$$

Because it is difficult to quantify the $HRh(CO)_4$ in the present study due to its weak signal, the following equation is used to replace the concentration of saturated $HRh(CO)_4$ with $[Rh_4(CO)_{12}]^{1/4}[H_2]^{1/2}[CO]^1$:

$$\mathrm{Rh_4(CO)_{12} + 2H_2 + 4CO \leftrightarrow 4HRh(CO)_4}. \quad (7)$$

Thus the new expression for the rate of hydroformylation in terms of observable organometallics becomes

$$\mathrm{rate} = k_1[\mathrm{RCORh(CO)_4}][\mathrm{CO}]^{-1}[\mathrm{H_2}] + k_2[\mathrm{RCORh(CO)_4}][\mathrm{Rh_4(CO)_{12}}]^{1/4}[\mathrm{H_2}]^{1/2}[\mathrm{CO}]^Y. \quad (8)$$

Dividing through by the acyl rhodium tetracarbonyl concentration provides the following working expression for the apparent TOF of aldehyde formation:

$$\mathrm{TOF_{total}} = k_1[\mathrm{CO}]^{-1}[\mathrm{H_2}] + k_2[\mathrm{Rh_4(CO)_{12}}]^{1/4}[\mathrm{H_2}]^{1/2}[\mathrm{CO}]^Y. \quad (9)$$

Again, the first term presents the classic unicyclic hydroformylation mechanism, and the second term is the contribution from the CBER. All of the experimental data at 298 K were used to regress the foregoing equation to provide the values

$$k_1 = (1.600 \pm 0.109) \times 10^{-2}\ \mathrm{s}^{-1},$$

$$k_2 = (5.603 \pm 1.143) \times 10^{-2}\ \mathrm{s}^{-1},$$

and

$$y = -(6.275 \pm 0.732) \times 10^{-1}.$$

To further evaluate the contribution of a CBER, we prepared a plot of the TOFs versus $[Rh_4(CO)_{12}]^{1/4}$ from the $Rh_4(CO)_{12}$ series of experiments (Fig. 7). Regression of all of the rhodium series data provided the following result:

$$\mathrm{TOF} = 0.00360 \pm 0.00030\ \mathrm{s}^{-1} + 0.03806 \pm 0.00328\ \mathrm{s}^{-1} \times[\mathrm{Rh_4(CO)_{12}}]^{0.25}, \quad (10)$$

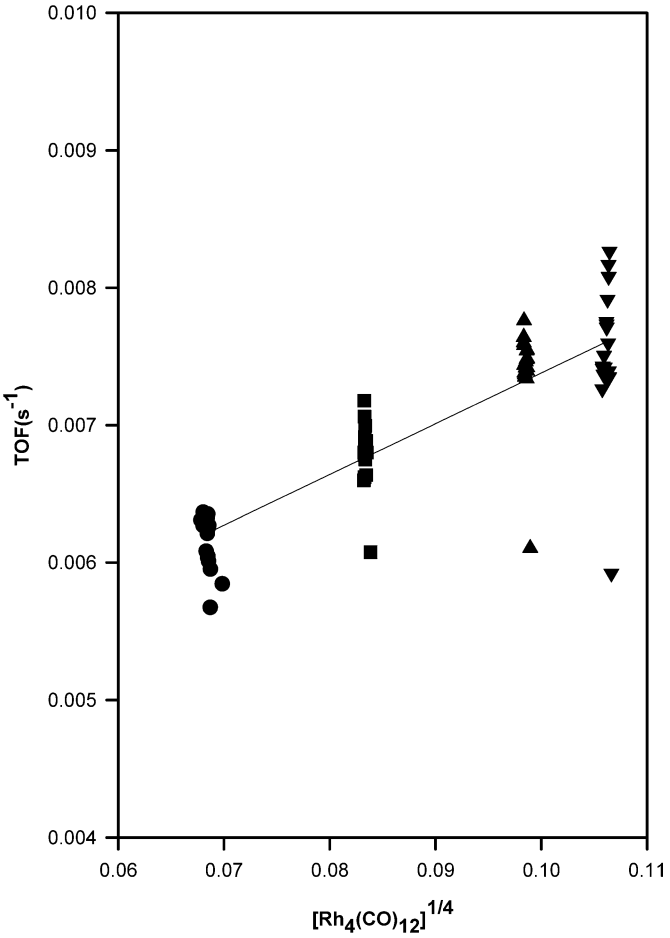

Fig. 7. The dependence of the instantaneous values of TOF on the instantaneous values of observable $Rh_4(CO)_{12}$ for the set of experiments with varying nominal rhodium concentration. The remaining reaction conditions are held constant at $V_{alkene} = 10$ mL, $P_{CO} = 4.0$ MPa, $P_{H_2} = 2.0$ MPa at 298 K.

where the errors are presented as twice the standard deviation. This indicates that the contributions of catalytic binuclear elimination are 36.7, 42.7, 47.7, and 48.6% at initial $Rh_4(CO)_{12}$ loadings of 52.60, 102.10, 199.80, and 253.30 mg, respectively. The lowest points in Fig. 7 represent the first measurements in each run and, as such, they represent outliers.

4. Discussion

4.1. Spectroscopic considerations

The in situ spectroscopic measurements and analyzes result in relatively good pure component spectra and concentration profiles for the organic substrate cyclooctene, the primary organic product cyclooctane carboxaldehyde, the organic ketone side product, the organometallic precursor $Rh_4(CO)_{12}$, and the primary organometallic intermediate $RCORh(CO)_4$. In addition, using BTEM and TFA made it possible to confirm the presence of observable quantities of $HRh(CO)_4$ during catalysis, but the signals were too weak to obtain accurate concentration profiles as a function of time. The unusually high atmospheric moisture content in these spectra was a significant factor contributing to limitations in both pure component spectral reconstructions and the concentration profiles.

4.2. Equilibrated $HRh(CO)_4$

The existence of a rapidly obtainable equilibrium between observable quantities of a rhodium carbonyl complex $[Rh_4(CO)_{12}]$ and observable quantities of $HRh(CO)_4$ at room temperature under noncatalytic experiments and relatively moderate syngas pressures has been firmly established [48]. The catalytic case is more complex. Marko et al. [63] observed that the rate of hydroformylation of cyclohexene starting with $Rh_6(CO)_{16}$ is proportional to the 1/6th power of the initial carbonyl concentration, that is, $[Rh_6(CO)_{16}]^{1/6}$. These data suggest an equilibrium between the hexanuclear rhodium carbonyl complex precursor and a mononuclear rhodium hydride during catalysis. Our work starting with $Rh_4(CO)_{12}$ as precursor and cycloalkenes as substrates showed that equilibrium-controlled precursor conversion occurs among the observable tetranuclear precursor, an unobservable mononuclear hydride, and the observable mononuclear rhodium acyl carbonyl [16]. The rate of cyclohexene hydroformylation starting with $Rh_4(CO)_{12}$ was proportional to the 1/4th power of the initial carbonyl concentration, that is, $[Rh_4(CO)_{12}]^{1/4}$. This was then shown to be a more general phenomenon, because equilibrium precursor conversion was also seen with other cyclic alkenes, including cyclooctene [20]. Rhodium carbonyl hydride was not observable in either of the aforementioned spectroscopic studies.

In the present study, the development of BTEM made it possible to detect $HRh(CO)_4$. Although equilibrium-controlled precursor conversion is seen in this system, and although $HRh(CO)_4$ must be in equilibrium exchange with the precursor, it was not possible to experimentally quantify the equilibrium. Again this was due to the weak signals involved and, more importantly, the unusually high atmospheric moisture content in the spectra and the resulting difficulties in obtaining good concentration profiles. Accordingly, it was necessary to model the equilibrium concentrations of $HRh(CO)_4$ in terms of the more accurate measurements of the instantaneous concentrations of $Rh_4(CO)_{12}$.

4.3. Kinetics and evidence for homometallic CBER

The classic unicyclic unmodified rhodium catalytic cycle must exist during the hydroformylation of cyclooctene as it does during the hydroformylations of other alkenes that have been modeled successfully [14–16]. Accordingly, the observable rate of hydroformylation must have a linear term in the total concentration of rhodium intermediates. Indeed, this is experimentally verified by the term $k_1[RCORh(CO)_4][CO]^{-1}[H_2]$. However, a second catalytic mechanism is operating simultaneously, arising from the attack of $HRh(CO)_4$ on the primary observable rhodium intermediate $RCORh(CO)_4$ [or, more appropriately, the coordinately unsaturated species $RCORh(CO)_3$]. This generates a second term in the rate expression involving the product $[RCORh(CO)_4][HRh(CO)_4]$. This term is quadratic

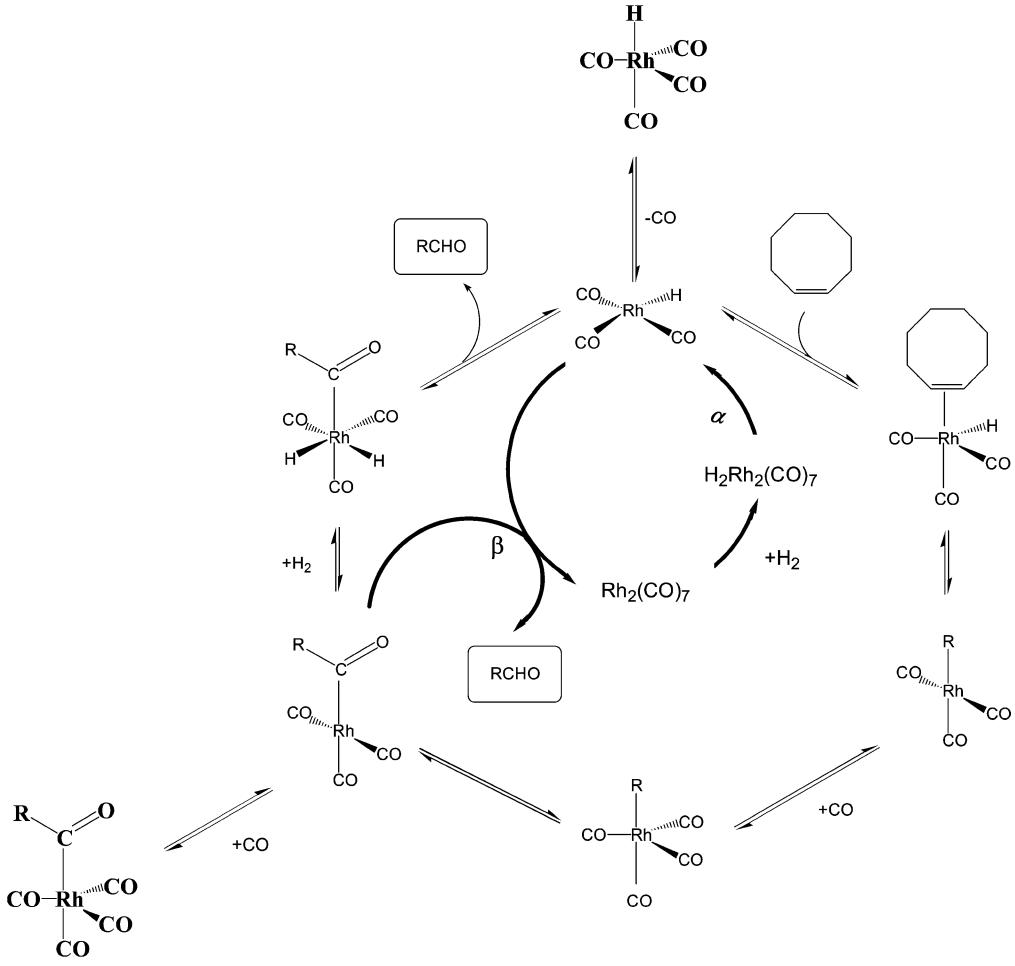

Scheme 1. Proposed reaction mechanism for the simultaneous interconnected unicyclic and homometallic CBER hydroformylation reactions. The species $HRh(CO)_4$ and $RCORh(CO)_4$, represented in bold type, are the observable organometallics under reaction conditions.

in rhodium. This second term accounts for the contribution of the homometallic CBER.

The topology of this interconnected catalytic rhodium system, consisting of both a unicyclic mechanism and homometallic CBER involving rhodium alone, and giving rise to linear-quadratic kinetics, is shown in Scheme 1.

It is possible, perhaps even probable, that the binuclear mechanism exists in many (or most) other hydroformylations of alkenes, including very reactive α-olefins. However, the experimentally determined kinetics probably will not indicate the presence of a statistically significant quadratic term in most of these systems due to the ultra-low steady-state concentrations of $HRh(CO)_4$ and hence low probability for CBER. In this study with cyclooctene, the quadratic term is statistically verifiable. It arises in large part due to the relatively high concentrations of $HRh(CO)_4$ present throughout the entire reaction period due to equilibrated conversion with the large pool of $Rh_4(CO)_{12}$ available.

4.4. Clarification of equilibrium-controlled precursor conversion

Equilibrium-controlled precursor conversion was first experimentally observed and successfully modeled for the case of $Rh_4(CO)_{12}$ as precursor in the hydroformylation of cyclohexene [16]. The hydroformylation kinetics are consistent only with a unicyclic catalytic reaction topology. Under this working assumption, a pseudo-steady-state hypothesis was posited for the concentration of $HRh(CO)_3$, and Eq. (3) was derived. The crucial equation for the pseudo-steady-state hypothesis is

$$\begin{aligned} &d[HRh(CO)_3]/dt \approx 0 \\ &\quad = k_i[RCORh(CO)_4][CO]^{-1}[H_2] \\ &\qquad - k_{ii}[Rh_4(CO)_{12}]^{1/4}[H_2]^{1/2}[\text{alkene}]. \end{aligned} \tag{11}$$

In the present contribution, the system has simultaneously one unicylic and one homo-bimetallic CBER reaction topology. Under this circumstance, there exists an extra term in the pseudo steady state hypothesis, namely that arising from the CBER contribution. The resulting equation is

$$\begin{aligned} &d[HRh(CO)_3]/dt \approx 0 \\ &\quad = k_i[RCORh(CO)_4][CO]^{-1}[H_2] \\ &\qquad - k_{ii}[Rh_4(CO)_{12}]^{1/4}[H_2]^{1/2}[\text{alkene}] \\ &\qquad + k_{iii}[RCORh(CO)_4][Rh_4(CO)_{12}]^{1/4}[H_2]^{1/2}[CO]^{-1}. \end{aligned} \tag{12}$$

Table 4
Comparison of unicyclic TOF for previous rhodium hydroformylations

Substrate	Metals used	TOF_{uni} (min^{-1})	Reaction topologies present	Reference
3,3-Dimethyl-but-1-ene	Rh	0.11[a]	Unicyclic	[15]
Cyclohexene	Rh	0.135[b]	Unicyclic	[16]
Styrene	Rh	0.056, 0.076[c]	Unicyclic	[17]
3,3-Dimethyl-but-1-ene	Rh, Mn	0.079[d]	Unicyclic and hetero-bimetallic CBER	[43]
Cyclopentene	Rh, Mn	0.12[e]	Unicyclic and hetero-bimetallic CBER	[44]
Cyclooctene	Rh	0.21[f]	Unicyclic	[20]

[a] At 293 K, 2.0 MPa CO, 2.0 MPa H_2 in *n*-hexane.
[b] At 293 K, 6.0 MPa CO, 2.0 MPa H_2 in *n*-hexane.
[c] Minor and major region-selective cycles at 298 K, 5.0 MPa CO, 0.5 MPa H_2 in *n*-hexane.
[d] At 298 K, 2.0 MPa CO, 1.0 MPa H_2 in *n*-hexane.
[e] At 289.7 K, 2.0 MPa CO, 2.0 MPa H_2 in *n*-hexane.
[f] At 298 K, 4.0 MPa CO, 2.0 MPa H_2 in *n*-hexane.

Therefore, in the case of a mixed unicyclic and CBER topology, the corrected expression for equilibrium precursor control is given by Eq. (13). Comparison with Eq. (1), which is strictly valid only for a unicyclic topology, shows that the anticipated observable orders for CO and alkene should remain the same, but that the orders of $Rh_4(CO)_{12}$ and H_2 shift. As the CBER hydroformylation contribution becomes very large compared with the unicyclic hydroformylation contribution, Eq. (13) becomes proportional to just the product [alkene][CO]. In the present set of experiments, the contribution of the CBER is at most only ca. 40% of the total aldehyde formation:

$$[\mathrm{RCORh(CO)_4}]_{SS} = k_{ii}[\mathrm{Rh_4(CO)_{12}}]_{SS}^{1/4}[\mathrm{H_2}]^{-1/2}[\text{alkene}][\mathrm{CO}] \Big/ \left(k_i + k_{iii}[\mathrm{Rh_4(CO)_{12}}]_{SS}^{1/4}[\mathrm{H_2}]^{-1/2}\right). \quad (13)$$

4.5. Comparison of unicyclic TOF to previous rhodium hydroformylations

The detailed kinetics of a few unmodified rhodium hydroformylation reactions (i.e., involving full rate expressions based on observable intermediates) have been determined using simultaneous in situ spectroscopic measurements. Table 4 lists the unicyclic TOFs determined from these studies. As Table 4 shows, the unicycle TOFs vary over a narrow range, regardless of the substrate used. In all of these studies, the functional form of the unicyclic TOF was the same, namely $[\mathrm{CO}]^{-1}[\mathrm{H_2}][\text{alkene}]^0$. In a previous comparative study with rhodium at ca. 6×10^{-5} mol fraction, involving homologous series of alkenes (i.e., cycloalkene, terminal linear alkenes, internal terminal alkenes, and methylene cycloalkanes), it was observed that all of the observed TOFs were ca. 0.04–0.20 min^{-1} measured at 293 K, 2.0 MPa CO, and 2.0 MPa H_2 in *n*-hexane. In addition, cyclooctene exhibited the highest TOF, at ca. 0.20 min^{-1} [20]. The present contribution is consistent with an elevated TOF for cyclooctene.

The issue of parametric sensitivity must be raised. First, regression of the data given in Fig. 7 assumes an exponent equal to 0.25 for $Rh_4(CO)_{12}$ so that good bounds are obtained for the rate coefficients. But this might impose a small bias, because the value of the unicyclic TOF is highly dependent on the exact value of the exponent. If the regression were performed once again with an exponent equal to 0.2, then we would obtain a TOF_{uni} equal to 0.0027 ± 0.0003 s^{-1} (i.e., 0.16 min^{-1}), which is more consistent with other systems. This reemphasizes the foregoing argument about parametric sensitivity. Finally, an extensive comparison between the TOF in this study and that obtained previously [20] is unnecessary, because the latter value of TOF was only a rough first approximation (determined from a single experimental run).

4.6. Other types of systems exhibiting nonlinear or quadratic terms

It is important to mention that a few other homogeneous catalytic systems are known to exhibit rates of reaction that are nonlinear or even quadratic in metal loading. The most studied systems involve ring-opening reactions of epoxides. For example, the asymmetric ring opening of epoxides with trimethyl azide catalyzed by $(\mathrm{Salen})\mathrm{Cr}^{III}$ complexes exhibited rates that are second order in chromium [64]. The proposed catalytic mechanism is in fact a monometallic CBER, because it involves mononuclear species and dinuclear species, in which the key step is the intermolecular reaction of two chromium complexes with Salen, epoxide and azide ligands. As far as we know, no detailed kinetic and mechanistic follow-up study has been published to date.

Detailed kinetic and mechanistic studies of related ring-opening reactions of epoxides using zirconium complexes and zinc complexes have appeared, however. Zirconium complexes of the $C3$-symmetric ligand (+)-(*S*,*S*,*S*)-triisopropanolamine as precursors have been shown to promote the stereoselective reaction of cyclohexene oxide and trimethyl azide, with a reaction order of ca. 0.5 in total zirconium observed [65]. The mechanism of this reaction is believed to involve a catalytic cycle with exclusively dimeric zirconium intermediates. In the case of zinc-diiminate-catalyzed copolymerization of cyclohexene oxide and CO_2, a reaction order of 1.0–1.8 in zinc was observed [66]. The mechanism of this reaction is believed to involve a catalytic cycle with exclusively dimeric zinc intermediates, but the possible existence of a simultaneous catalytic cycle with exclusively mononuclear zinc intermediates was also considered.

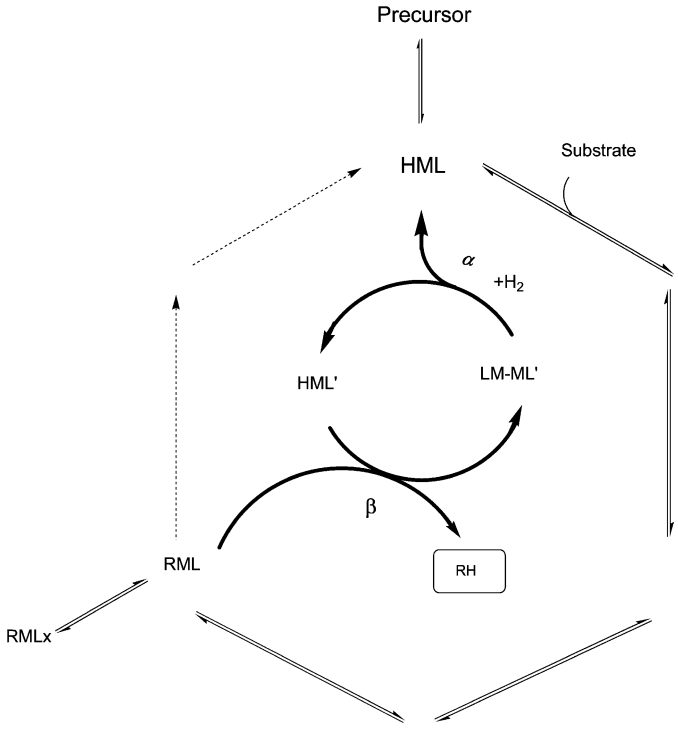

Scheme 2. Proposed reaction topology for homometallic CBER with purely quadratic kinetics.

4.7. Metal utilization and synthetic efficiency

In the present contribution, the quadratic effects to the overall rate of product formation increases only slowly as the nominal metal concentration is increased. This is due to the fact the precursor is tetranuclear and its conversion is equilibrium-controlled. Such a situation is particularly disadvantageous. Systems with mononuclear precursors controlled by equilibrium conversion will show significantly more pronounced rate increases as a function of total metal loading.

Increasing the nominal metal loadings in small-volume syntheses provides a means of using the metal complexes in a far more efficient manner. Practical reaction engineering limits to such endeavors would soon be encountered as loading is increased, including (i) the solubility limits of the precursor/intermediates under reaction conditions, (ii) possible gas–liquid mass transfer limitations, and (iii) the limited heat transfer capacity of the reactor configuration. As the nominal metal loading increased, the contribution of a unicyclic mechanism would decrease.

4.8. Generating a homometallic CBER with purely quadratic kinetics

It is interesting to consider the possibilities and prerequisites for a homometallic CBER that would exhibit purely quadratic kinetics in organometallic species. Restricting ourselves to catalytic reactions involving hydride species, we can image a situation similar to that shown in Scheme 1. As shown in Scheme 2, the metal, M, is modified with a ligand, L, and this modified hydride, HML, can react with substrate. However, further molecular hydrogen activation on RML proves difficult. At the same time, another hydride species, HML′, with ligand L′, is also present in solution, but this species does not readily undergo reaction with substrate. The homometallic CBER would dominate the catalytic kinetics, because step β dominates, and a higher-order utilization of the metal would be achieved. (It is implicitly understood that the hydrogen activation [step α] must be efficient.) To avoid ligand exchange, L, L′, or both may be (or should be) nondissociating.

A qualifying statement needs to be made regarding the generalized kinetics of Schemes 1 and 2. The kinetic polynomial governing a homometallic CBER would by itself have a linear-quadratic form. The quadratic term controls the kinetics when the mononuclear species are predominant and the dinuclear species are minor, and thus the rate-determining step is bimolecular elimination. At very high metal loadings and low rates α, a shift in species distribution is possible to predominantly dinuclear species with mononuclear species as minor species. In this limit, hydrogen activation is rate-controlling, and the linear kinetic term dominates.

5. Conclusion

The present study has identified a catalytic system that exhibits linear-quadratic kinetics. These linear quadratic kinetics arise from a simultaneous unicyclic mechanism and a homometallic CBER. The homometallic CBER contributes a significant amount (40%) of the reaction product. Identifying the mechanistic reasons for system activity required detailed and quantitative in situ spectroscopic measurements. The implications of CBER include a rationale for nonlinear kinetic effects that differs from those in many previously proposed mechanisms. This study has also provided further insight into equilibrium-controlled precursor conversion.

Acknowledgments

Financial support for this experimental research was provided by the Academic Research Fund of the National University of Singapore (NUS). Research scholarships for GL and LG were provided by the Graduate School of Engineering (NUS). CL thanks Singapore Millennium Foundation (SMF) for a postdoctoral fellowship. The authors thank Ferenc Ungvary, Jack Norton, and Istvan Kovacs for the valuable discussions.

Supporting information

Plots of $RCORh(CO)_4$ versus time, RCHO versus time, and TOF versus time for the experimental series involving CO variation, hydrogen variation, cyclooctene, and temperature are available free of charge at DOI:10.1016/j.jcat.2005.09.033.

References

[1] C.D. Frohning, C.W. Kohlpaintner, in: B. Cornils, W.A. Herrmann (Eds.), Applied Homogeneous Catalysis with Organometallic Compounds: A Comprehensive Handbook, vol. 1, Wiley–VCH, Weinheim, 1996, chap. 2.

[2] P.C.J. Kamer, J.N.H. Peek, P.W.N.M. van Leeuwen, in: B. Heaton (Ed.), Mechanism in Homogeneous Catalysis, Wiley–VCH, Weinheim, 2005, p. 231.
[3] J. Falbe, New Syntheses with Carbon Monoxide, Springer, New York, 1980.
[4] H. Adkins, G. Kresk, J. Am. Chem. Soc. 70 (1948) 383.
[5] G. Schiller, Ger. Pat. 953,605, 1956.
[6] E.L. Jenner, R.V. Lindsey, US Patent 2,876,254, 1959.
[7] P. Pino, F. Piacenti, M. Bianchi, in: L. Wender, P. Pino (Eds.), Org. Synth. Met. Carbonyls, vol. 2, Wiley, New York, 1977, pp. 233–296.
[8] J. Palagyi, G. Palyi, L. Marko, J. Organomet. Chem. 14 (1968) 238.
[9] G. Csontos, B. Heil, L. Marko, Ann. N.Y. Acad. Sci. 239 (1974) 47.
[10] A. Sisak, F. Ungvary, L. Marko, Organometallics 2 (1983) 1244.
[11] L. Marko, F. Ungvary, J. Organomet. Chem. 432 (1992) 1.
[12] F. Ungvary, Coord. Chem. Rev. 170 (1998) 245.
[13] F. Ungvary, Coord. Chem. Rev. 218 (2001) 1.
[14] M. Garland, G. Bor, Inorg. Chem. 28 (1989) 410.
[15] M. Garland, P. Pino, Organometallics 10 (1990) 1693.
[16] C. Fyhr, M. Garland, Organometallics 12 (1993) 1753.
[17] J. Feng, M. Garland, Organometallics 18 (1999) 417.
[18] G. Consiglio, B. Studer, F. Oldani, P. Pino, J. Mol. Catal. 58 (1990) L9.
[19] C. Li, L. Guo, M. Garland, Organometallics 23 (2004) 2201.
[20] G. Liu, R. Volken, M. Garland, Organometallics 17 (1999) 3429.
[21] J.A. Osborn, F. Ardine, J. Young, G. Wilkinson, J. Chem. Soc. Am. 12 (1966) 1711.
[22] K.H. von Brandes, H.B. Jonassen, Z. Anorg. Allg. Chem. 343 (1966) 215.
[23] F. Ungvary, L. Marko, J. Organomet. Chem. 20 (1969) 205.
[24] B.H. Byers, T.L. Brown, J. Am. Chem. Soc. 99 (1977) 2528.
[25] D.S. Breslow, R.F. Heck, Chem. Ind. (London) (1960) 467.
[26] F. Ungvary, L. Marko, Organometallics 2 (1983) 1608.
[27] I. Kovacs, F. Ungvary, L. Marko, Organometallics 5 (1986) 209–215.
[28] C. Hoff, F. Ungvary, R.B. King, L. Marko, J. Am. Chem. Soc. 107 (1985) 666.
[29] J. Norton, W. Carter, J. Kelland, S. Okrasinski, Adv. Chem. Ser. 167 (1978) 170.
[30] J. Norton, Acc. Chem. Res. 12 (1979) 139.
[31] R.T. Edidin, K. Hennessy, A. Moody, S. Okrasinski, J. Norton, New J. Chem. 12 (1988) 475.
[32] M.J. Nappa, R. Santi, S. Diefenbach, J. Halpern, J. Am. Chem. Soc. 104 (1982) 619.
[33] M.J. Nappa, R. Santi, J. Halpern, Organometallics 4 (1985) 34.
[34] I. Kovacs, C.D. Hoff, F. Ungvary, L. Marko, Organometallics 4 (1985) 1347.
[35] C.K. Brown, D. Georglou, G. Wilkinson, J. Chem. Soc. A (1971) 3120–3127.
[36] J. Schwartz, J. Cannon, J. Am. Chem. Soc. 96 (1974) 4721.
[37] B. Martin, D.K. Warner, J. Norton, J. Am. Chem. Soc. 108 (1986) 33.
[38] J.C. Barborak, K. Cann, Organometallics 1 (1982) 1726.
[39] W.D. Jones, R.G. Bergmann, J. Am. Chem. Soc. 79 (1979) 5447.
[40] W.D. Jones, J. Huggins, R.G. Bergman, J. Am. Chem. Soc. 103 (1981) 4415.
[41] N.H. Alemdaroglu, J.L.M. Penninger, E. Oltay, Monatsh. Chem. 107 (1976) 1153.
[42] M.F. Mirbach, J. Organomet. Chem. 265 (1984) 205.
[43] J.P. Collman, J. Belmont, J. Brauman, J. Am. Chem. Soc. 105 (1983) 7288.
[44] J. Feng, M. Garland, Organometallics 18 (1999) 1542.
[45] M. Garland, in: B. Heaton (Ed.), Mechanism in Homogeneous Catalysis, Wiley–VCH, Weinheim, 2005, p. 151.
[46] W. Chew, E. Widjaja, M. Garland, Organometallics 21 (2002) 1882.
[47] E. Widjaja, C. Li, M. Garland, Organometallics 21 (2002) 1991.
[48] C. Li, E. Widjaja, W. Chew, M. Garland, Angew. Chem. Int. Ed. 20 (2002) 3785.
[49] C. Li, E. Widjaja, M. Garland, J. Catal. 213 (2003) 126.
[50] E. Widjaja, C. Li, W. Chew, M. Garland, Anal. Chem. 75 (2003) 4499–4507.
[51] E. Widjaja, C. Li, M. Garland, J. Catal. 223 (2004) 278.
[52] C. Li, E. Widjaja, M. Garland, J. Am. Chem. Soc. 18 (2003) 5540.
[53] C. Li, E. Widjaja, M. Garland, Organometallics 23 (2004) 4131.
[54] G. Liu, Kinetics and mechanism study of homogeneous hydroformylation, M. Eng. Thesis, National University of Singapore, 1999.
[55] D.F. Shriver, M.A. Drezdzon, The Manipulation of Air-Sensitive Compounds, Wiley, New York, 1986.
[56] A. Haynes, in: B. Heaton (Ed.), Mechanism in Homogeneous Catalysis, Wiley–VCH, Weinheim, 2005, p. 107.
[57] L. Damoense, M. Datt, M. Green, C. Steenkamp, Coord. Chem. Rev. 248 (2004) 2393.
[58] M. Garland, in: I.T. Horvath (Ed.), Transport Effects in Homogeneous Catalysis, Encyclopedia of Catalysis, Wiley, New York, 2002.
[59] R. Whyman, In Situ Spectroscopic Studies in Homogeneous Catalysis, Adv. Chem. Ser., Homogeneous Transition Met. Catal. React. 230 (1992) 19–31.
[60] J.L. Vidal, W.E. Walker, Inorg. Chem. 20 (1981) 249.
[61] E.R. Malinowski, Factor Analysis in Chemistry, Wiley, New York, 1991.
[62] G. Liu, M. Garland, J. Organomet. Chem. 608 (2000) 76.
[63] G. Csontos, B. Heil, L. Marko, Ann. NY Acad. Sci. 239 (1974) 47.
[64] K.B. Hansen, J.L. Leighton, E.N. Jacobsen, J. Am. Chem. Soc. 118 (1996) 10924.
[65] B.W. McCleland, W.A. Nugent, M.G. Finn, J. Org. Chem. 63 (1998) 6656.
[66] D.R. Moore, M. Cheng, E.B. Lobkovsky, G.W. Coates, J. Am. Chem. Soc. 125 (2003) 11911.